Table of Links

Task 1 Workplan

Task 1 examined magnetic flux leakage (MFL) for detection of mechanical damage defects. It evaluated existing signal generation and analysis methods to establish a baseline from which today's tools can be evaluated and tomorrow's advances measured, and it developed improvements to signal analysis methods and verified them through pull rig testing. Finally, it has built an experience base and defect sets to generalize the results from individual tools and analysis methods to the full range of practical applications. Many of the results from Task 1 will be further verified and developed under pressurized conditions as part of Task 3 of this project.

The focus in Task 1 was on MFL technology because MFL has successfully found metal-loss corrosion under a wide variety of conditions and it has found some mechanical damage under limited conditions. In addition, prior work showed that MFL can be enhanced to be sensitive to most types of mechanical damage. This sensitivity brings along technical difficulties, including more signals from benign conditions in the pipeline and increased system complexity. Many of these difficulties were addressed in Task 1.

Task 1 consisted of seven subtasks. These subtasks were planned to collect data with regard to detection of mechanical damage. Characterization, or determining the severity of the damage, was of interest but was not the main focus of the Task 1 work.

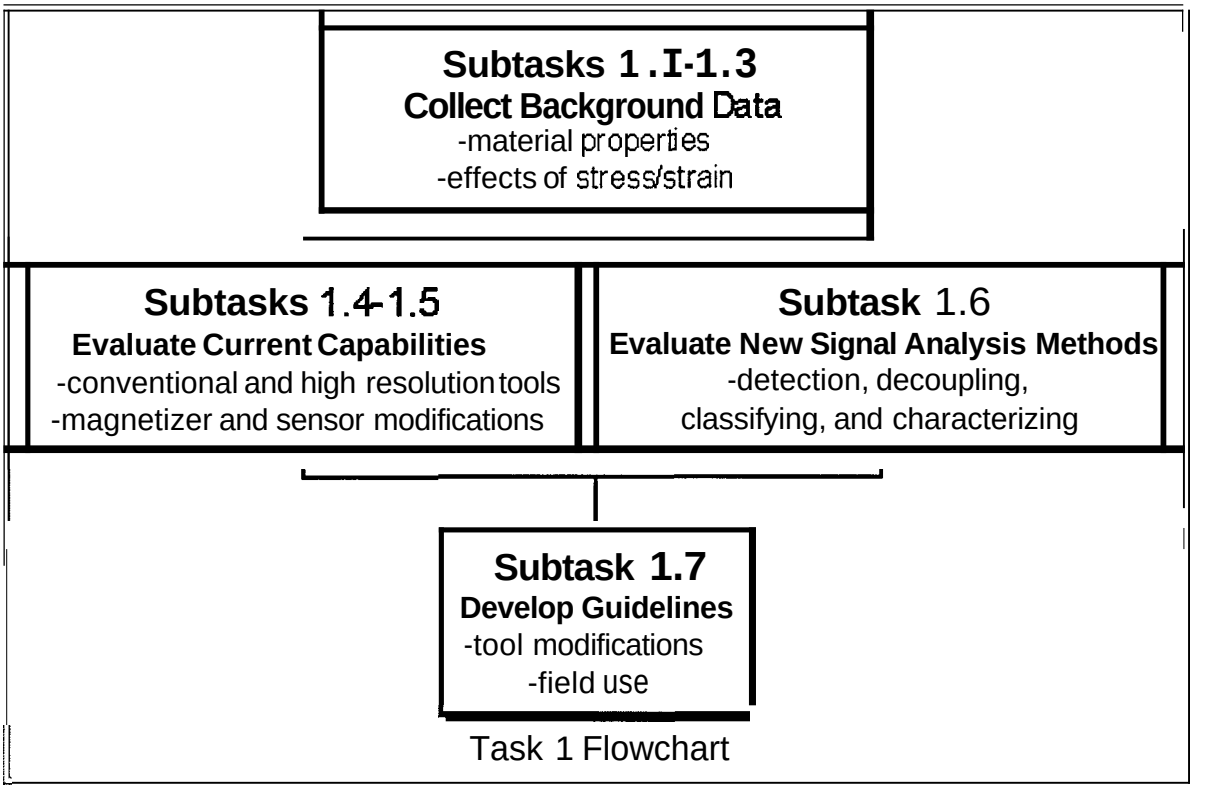

Task 1 Flowchart

Subtasks 1.1 to 1.3 collected background information to assess and develop signal analysis techniques and to provide data for extending prior experience:

- In Subtask 1.1, we measured the effects of mechanical damage on the magnetic properties of pipeline steels.
- In Subtask 1.2, we calculated the stress and strain conditions around mechanical damage (dent and gouge) defects.
- In Subtask 1.3, we collected data on the effects of magnetization level, velocity, and other parameters on measured MFL signals from mechanical-damage defects. Included here was limited testing under pressurized flowing conditions.

Subtasks 1.4 and 1.5 evaluated the capabilities of current inspection tool configurations and signal analysis techniques:

- In Subtask 1.4, we evaluated analysis methods used in conventional inspection equipment.
- In Subtask 1.5, we investigated changes in magnetizer and sensor arrangements to improve inspection results. In Subtask 1.5, we also evaluated the potential of new mechanical-damage tool configurations and analysis methods to increase the capabilities of in-line inspection for mechanical damage.

Subtasks 1.6 and 1.7 developed and evaluated the potential of future signal analysis methods and developed guidelines for using in-line inspection to reliably detect mechanical-damage defects:

- In Subtask 1.6, we evaluated full-signal analysis methods, such as neural networks.
- In Subtask 1.7, we generated guidelines for using in-line inspection equipment to increase the likelihood that mechanical-damage defects are found.

As the project continued, several changes were made to the work plan. Most notably, the original work plan called for nine mechanical finite-element analyses, which were then to be used as input to nine magnetic finite-element analyses. The goal of this effort was to understand how magnetic signals were produced at mechanical damage sites. In performing the mechanical finite-element analyses, we experienced difficulties with the computer code, which prevented us from completing the mechanical analyses. However, the results that we were able to obtain provided insightful information about defect stresses and strains. As a result, we increased the number of magnetic analyses and reduced the number of mechanical analyses.

Task 2 Workplan

Task 2 evaluated two inspection technologies for detecting cracks. The focus in Task 2 was on electromagnetic techniques that have been developed in recent years and that could be used on or as a modification to existing MFL tools. Ultrasonic techniques, while valuable, were not considered because they are the subject of research and development in ongoing GRI programs. Three subtasks were conducted to evaluate velocity-induced remote-field techniques, remote-field eddy-current techniques, and external techniques for sizing stress-corrosion cracks.

These subtasks were:

- Subtask 2.1. External Techniques for Sizing Stress-Corrosion Cracks.
- Subtask 2.2. Velocity-Induced Remote-Field Techniques.
- Subtask 2.3. Remote-Field Eddy-Current Techniques.

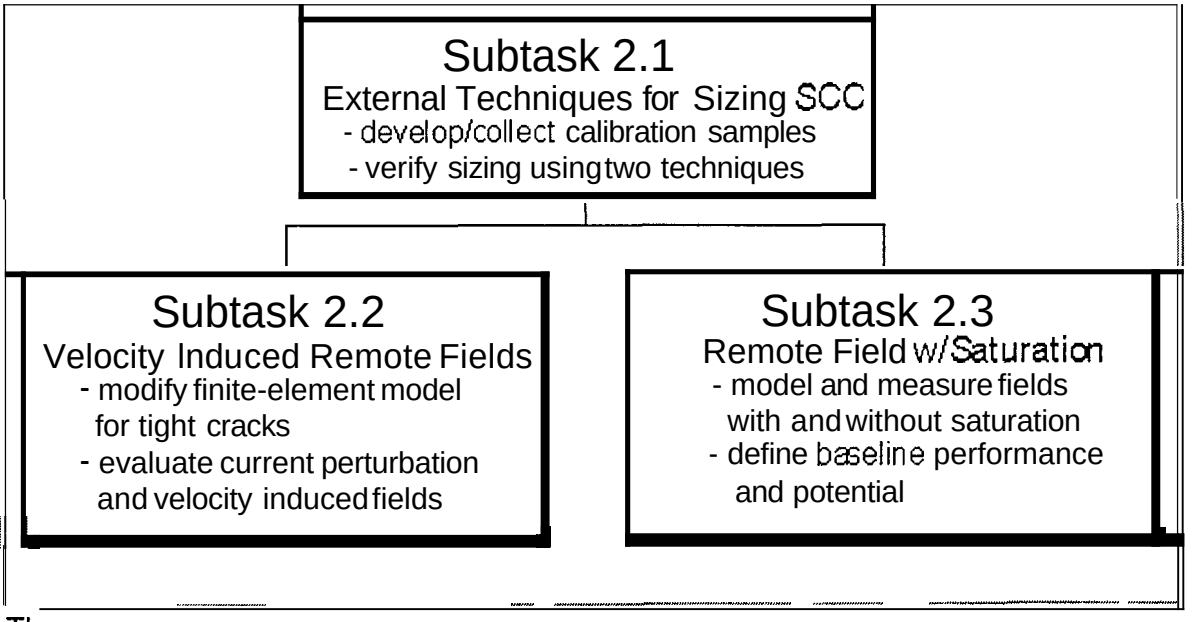

Th
the project.

Task 3 Workplan

Tasks 1 and 2 concentrated on developing methodologies for detecting and identifying mechanical damage and cracks. These methodologies were developed using laboratory tests, pull-rig tests, and analyses. Under Task 3, they were verified under realistic pressurized and flowing pipeline conditions. In addition, Task 3 sought to answer two important questions: Once a possible defect has been detected, how severe is the defect and is it likely to threaten the integrity of a pipeline?

The effects of pressure and operating conditions are particularly important. Pressure affects MFL signals by introducing stresses, which we affects MFL signals at mechanical damage. Also, operating conditions inside a pipeline are rugged, which makes application of sensor technologies difficult. Verifying and extending the results from unpressurized conditions to realistic pressurized conditions was considered essential to learning how to better apply the results of the first two years of this program to inspection tools.

Task 3 consisted of four subtasks:

- SubTask 3.1. Flow loop tests *to* determine the effects of stress and pressure on mechanical damage signals and calibrate the prior results taken under unpressurized conditions
- SubTask 3.2. Analyses to extend the previously developed detection algorithms to account for pressure
- SubTask 3.3. Development of techniques to measure stress and determine the severity of mechanical damage and cracks.
- SubTask 3.4. Final reporting.

Background Material on MFL

The magnetic flux leakage (MFL) response to pipeline anomalies depends on many things, including the magnetic properties of pipeline steel and the geometry of the defects. Magnetic flux inspection tools locate pipeline defects by applying a magnetic field in the pipe wall and then sensing a local change in this applied field. As an example of this process, corrosion changes the ferromagnetic pipe steel into non-ferromagnetic iron oxide. An MFL inspection tool detects this change in magnetic property because it reduces the local ability of the pipe to carry magnetic flux.

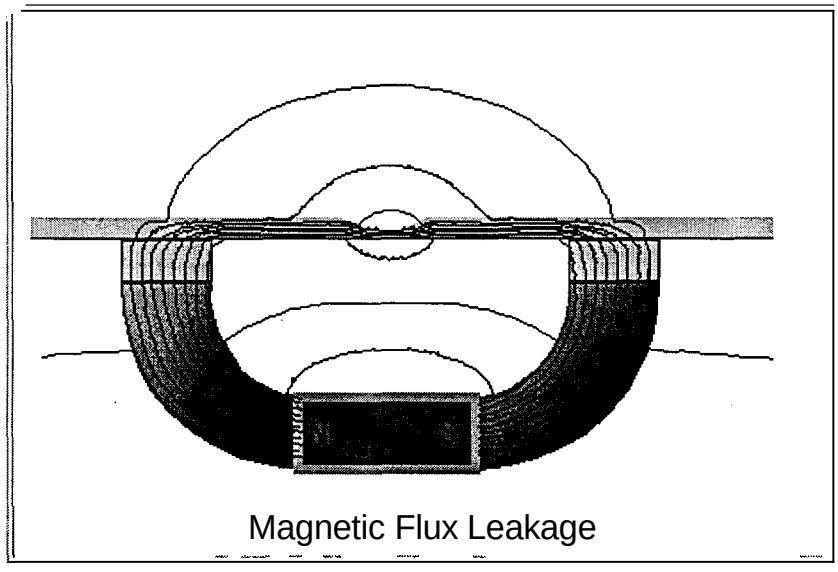

Magnetic Flux Leakage

Detecting mechanical damage works on the same principle, but the changes in magnetic properties are more subtle. For mechanical damage defects, the flux leakage is due to a change in magnetic property induced by stress and plastic deformation rather than removed metal. These changes are much smaller and depend on the pipeline steel and the damage characteristics.

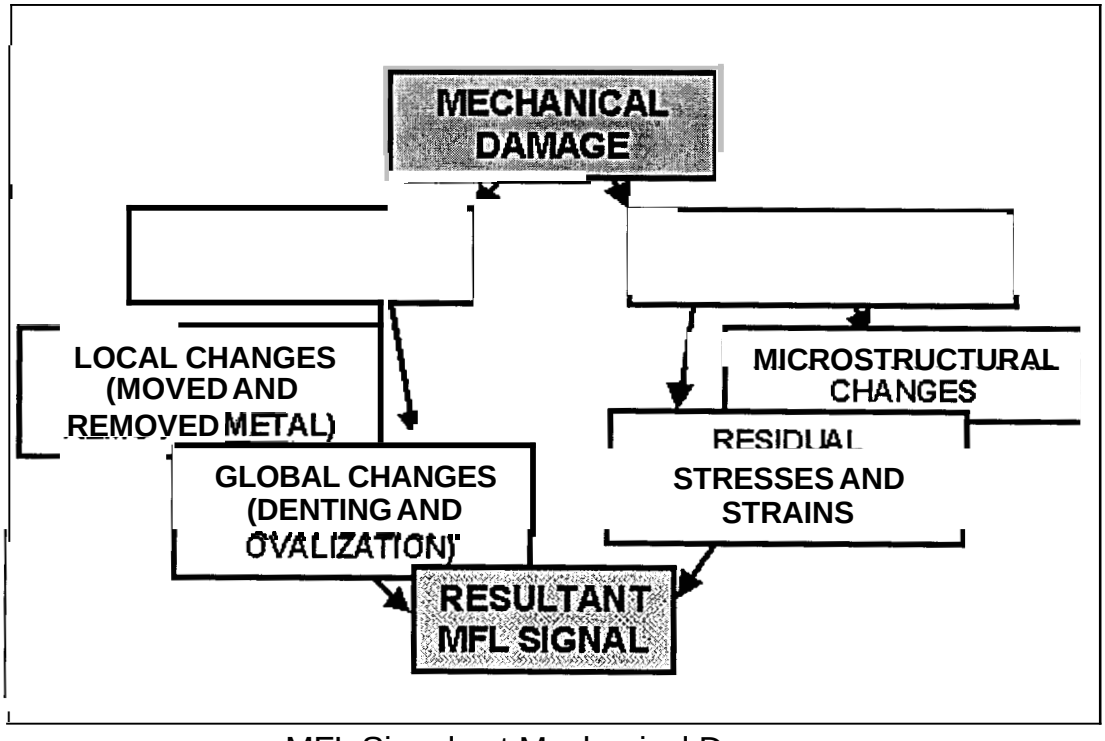

MFL Signals at Mechanical Damage

For more information on MFL, please refer to " Magnetic Flux Leakage (MFL) Technology for Natural Gas Pipeline Inspection"

Background Material on Magnetic Properties

The following figure shows a typical magnetization or B-H curve for a pipe material. As the applied magnetization level (H) increases, the flux density (B) in the pipe increases. At the knee of the magnetization curve, the slope changes abruptly and it continues to fall as the applied magnetization increases.

An MFL tool applies the magnetic field H to create the flux density B in the pipe, which can "leak" from the pipe material at defects. The relationship between the magnetic field and the flux density is nonlinear and hysteretic. Magnetization curves quantify the basic magnetic properties of ferromagnetic materials. These curves relate the applied magnetic field to the flux density in the material.

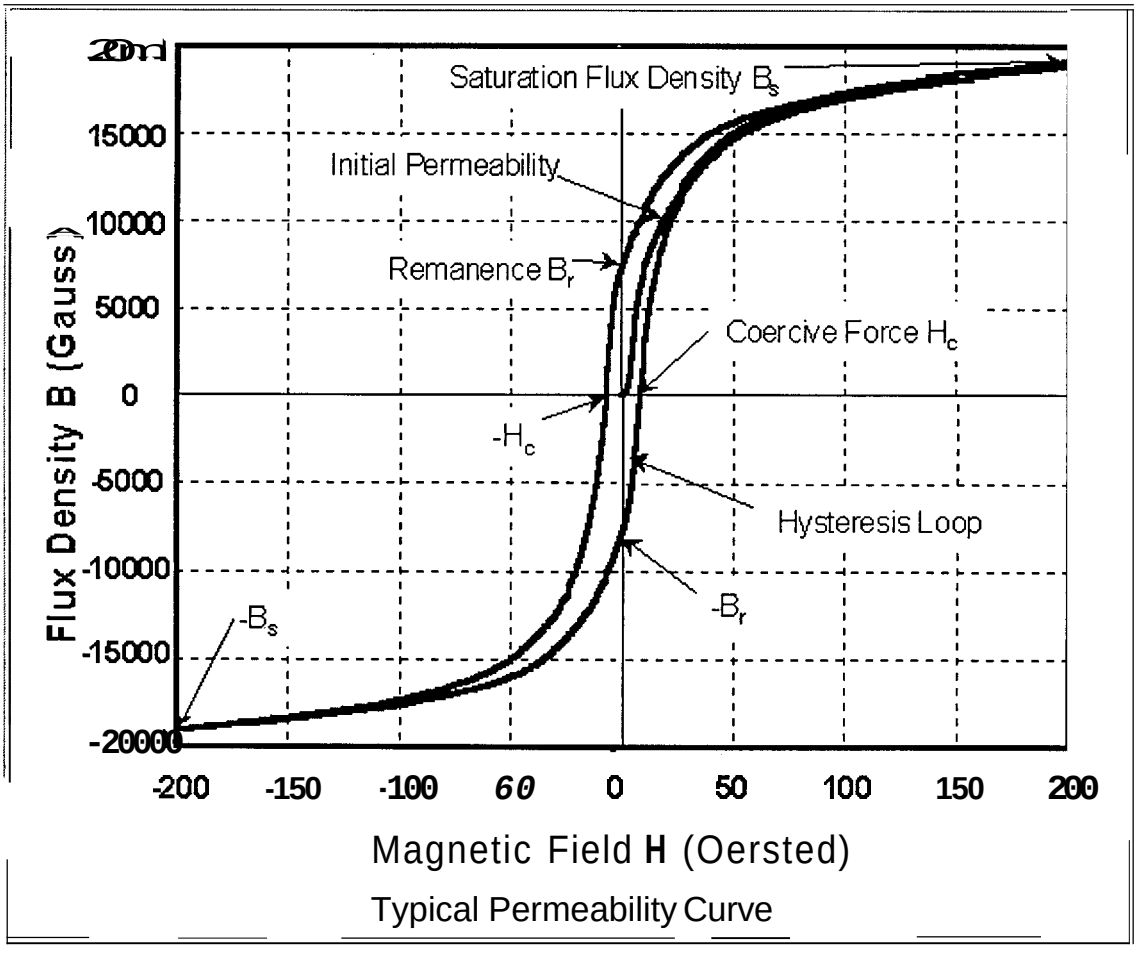

Typical Permeability Curve

B-H curves have two parts, the initial permeability and the hysteresis loop. Two commonly used measures, the coercive force (H_c) and the remanence (B_r), quantify the extent of the hysteresis. The coercive force is the direct current (DC) magnetizing field required to restore the magnetic flux density to zero after the

material has been magnetized. The remanence is the magnetic flux density measured while no magnetic field is applied. When the magnetization field is cycled at saturation levels, two additional measures are defined: the coercivity (H_{cs}) and the saturation remanence (B_{rs}). Both are the maximum values that can be attained after the material has been magnetized to saturation

Two other common magnetic properties are the saturation flux density (B_s), and DC permeability. These properties further characterize the overall B-H curve. The saturation flux density has many practical and technical definitions. In this work, the saturation flux density is fundamentally defined as the flux density where changes in hysteresis behavior are negligible with changes in magnetizing field and arbitrarily defined as the flux density at a magnetic field of 200 Oersted. The DC permeability is a generic term used to represent the ratio of the magnetic flux density to the magnetic field. In this work, the incremental permeability (i.e., the slope of the magnetization curve) is used. The incremental permeability is the ratio of the change in magnetic flux density to the change in magnetic field (i.e., B/H).

For more detailed information on the magnetic properties of pipeline steels, refer to Variation of Magnetic Properties in Pipeline Steels.

Background Material on Magnetic Property Changes with Stress and Strain

The magnetic properties of pipeline steels are variable and a function of fabrication process, alloying agents, and microstructure. Stress and strain play major roles in defining a steel's magnetic properties. Previous work by SwRI and Battelle measured the effects of stress on a small set of pipe samples, but the effects of plastic deformation were not measured.

The following figure shows a typical magnetization curve or B-H curve for a pipe material. As the applied magnetization level (H) increases, the flux density (B) in the pipe increases. At the knee of the magnetization curve, the slope changes abruptly and it continues to fall as the applied magnetization increases.

Adding stress or strain changes the shape of the magnetization curve. Compressive stress shifts the curve upward in the region of the knee, but it has little effect for higher magnetization levels. As a result, an MFL signal at a mechanical damage defect changes with magnetization level. At very high levels, there is almost no effect of stress and the signal is primarily due to the geometry of the defect. At low levels, the signal has both geometric and stress components.

Pipe grade, such as **API** grade X52, is not a measure of magnetic properties. Many fabrication processes and concentration of alloying elements can produce pipe of a particular grade but with different magnetic properties. Depending on the fabrication process, the magnetic properties can be anisotropic and **a** function of circumferential location with respect to the longitudinal seam weld.

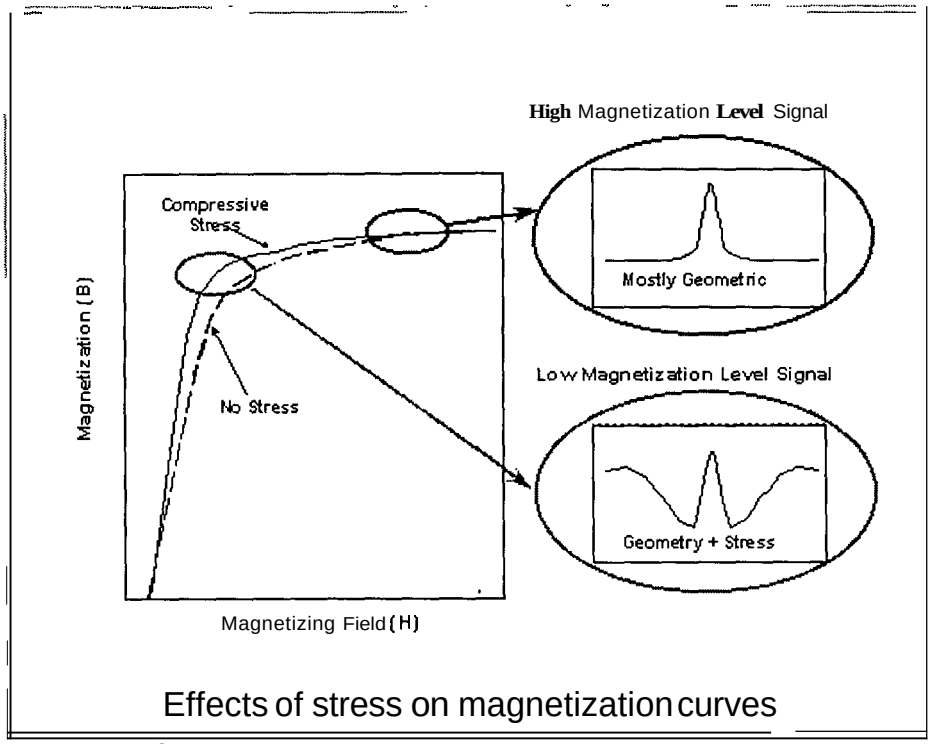

Effects of stress on magnetization curves

For more detailed information on the magnetic properties of pipeline steels, refer to "Variation of Magnetic Properties in Pipeline Steels"

Description of Typical Mechanical Damage Features

Mechanical damage is the largest cause of failures on gas-transmission pipelines today and a leading cause of failures on liquid lines. After a pipeline has been built, construction equipment (usually operated by outside parties) can deform the shape of a pipe, scrape away metal and coating, and change the mechanical properties of the steel. Sometimes this damage leads to immediate failure, and occasionally the damage leads to delayed or time-dependent failure. Obviously, immediate failures cannot be detected by periodic inspections. Consequently, a goal of this project is to detect those defects that might lead to delayed failure and differentiate them from benign defects.

Mechanical damage shows a number of features, such as:

(1) Denting

(2) Removal of metal at the surface of the pipe

(3) Cold-work of the material below the surface of the pipe and possible cracking in this area when the pipe is re-rounded by internal pressure

(4) Residual stresses and strains due to plastic deformation of the pipe wall

(5) Coating damage.

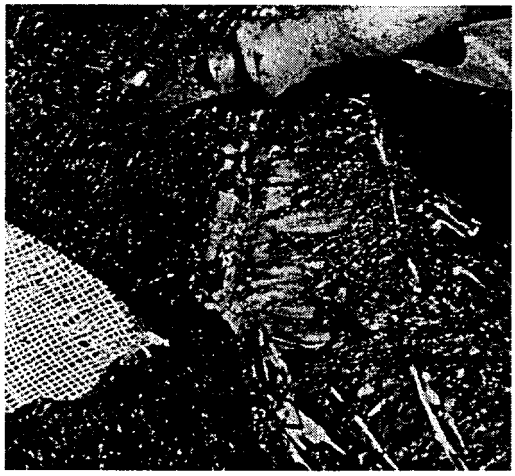

Mechanical Damage

The most significant of these features from the perspective of defect severity and the likelihood of delayed failure are the size and extent of the cold worked region. Dent depth, which can be easily measured by specific inspection tools, is not the most important parameter and is not sufficient to determine the severity of a mechanical damage defect. Movement or removal of metal by itself is usually not critical unless the

amount of metal affected is more than about 10 percent of the wall thickness. Of course, removal or movement of metal is usually accompanied by cold working, so the presence of changes in wall thickness could indicate a significant defect.

Comparison *of* MFL Signals for Metal Loss, Dents, and Cold Work

MFL is capable of detecting mechanical damage components such as simple dents, cold work, residual stresses/strains, and removed metal. Part of the signal generated at a mechanical damage defect is due to geometric changes - for example, a reduction in wall thickness due to metal loss causes flux to leak out. Some of the signal is due to the separation of the sensor from the pipe (lift-off), which can be minimized by a good sensor carrier system. The rest of the signal is largely due to magnetic changes, for example, changes in magnetization properties that result from stresses, strains, or damage to the microstructure of the steel.

MFL signals for metal loss, dents, cold work, residual stresses, and plastic strains are fundamentally different. These differences can be seen in the experimental MFL signals shown below. The signals correspond to the axial component of the MFL field as measured by a Hall-effect sensor.

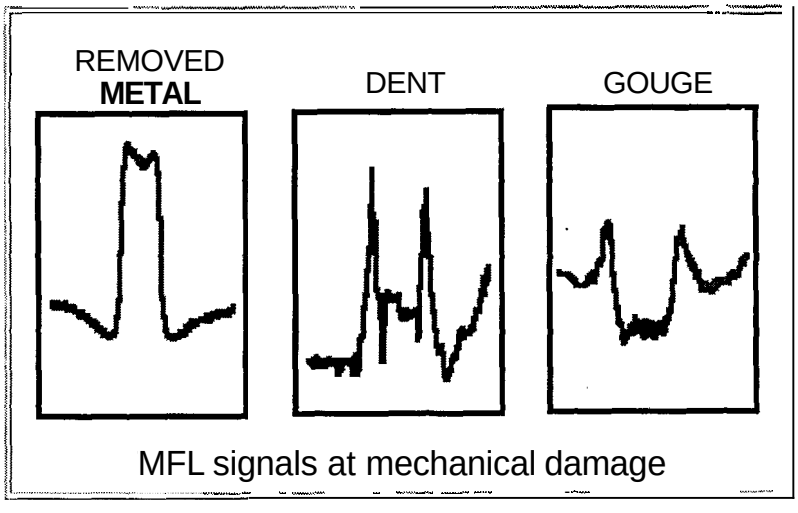

MFL signals at mechanical damage

The plot on the left is a typical MFL signal from metal loss. Flux, which is normally carried by the pipe wall, "leaks" in regions where the wall thickness is reduced. The sensor records an increase in flux level at the reduced-thickness area. Metal loss signals have a characteristic increase in measured field along the defect, with a slight decrease at both ends. For very long defects, there can be a dip in the signal in the center part of the defect.

The plot in the center is a typical MFL signal from a dent. Here, the signal shape is fundamentally different than that seen at metal loss. The signal is due to two effects that occur at the same time. First, the sensor orientation relative to the local pipe wall changes. The sensor still records the axial field but the pipe wall is no longer parallel to the sensor; since the flux field is a vector quantity, the resultant measurement changes. Second, residual stresses and strains change the local magnetic properties. Dent

signals show characteristic peaks near the start and finish of the dent with a relatively low signal through the defect.

The plot on the right is a typical MFL signal from a cold worked region. Here, the signal shape is fundamentally different from that of both metal loss or a dent. Flux in the region immediately below the cold worked area decreases. This change occurs because the cold worked region, which is on the side opposite the sensor, carries more flux, thereby reducing the flux in the rest of the pipe. In addition, there is a slight increase in signal at either end. These two signal features are characteristic of mechanical damage.

For more detailed information on MFL signals from mechanical damage, refer to "The Feasibility of Magnetic Flux Leakage In-line Inspection as a Method to Detect and Characterize Mechanical Damage."

Linear Test Rig Description

The linear test rig is a moveable platform for testing inspection technologies, including MFL systems, at typical inspection velocities. The inspection platform is pulled along a 24-foot guide rail either through a full diameter pipe or under a partial diameter pipe section. Tests conducted under this program used flat plates or a partial diameter pipe section that represented an arc of approximately 120 degrees.

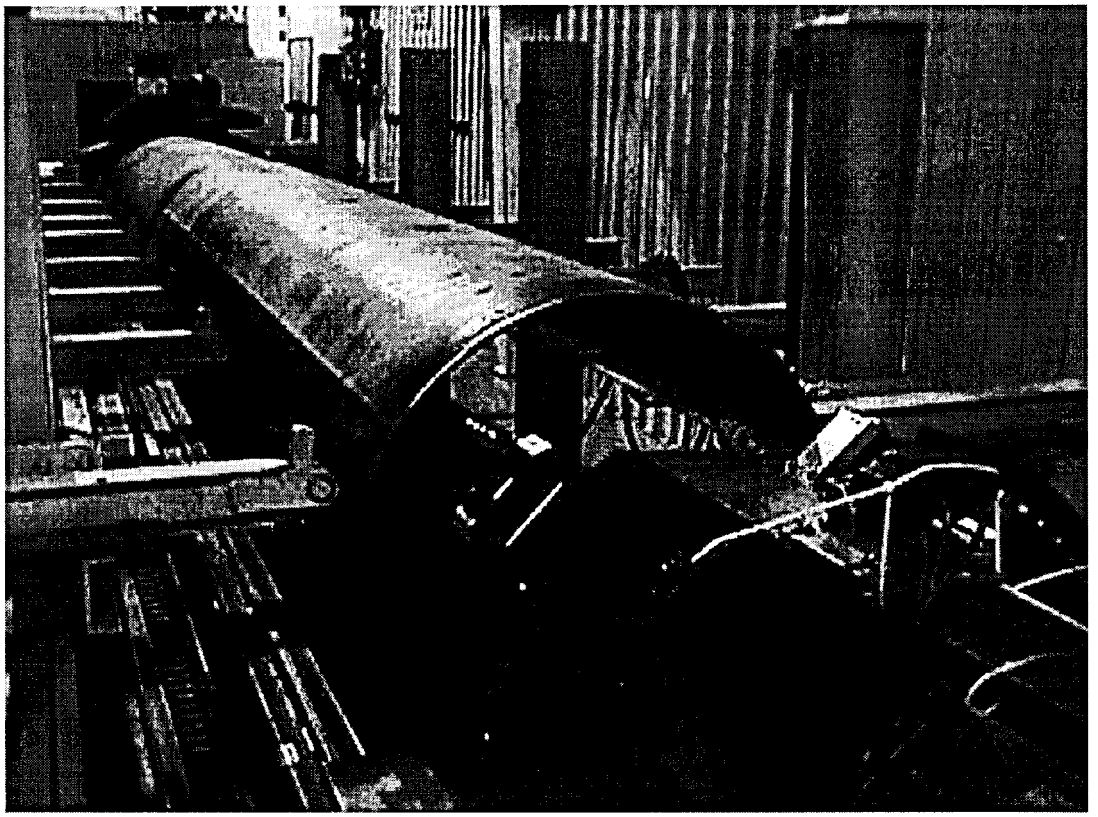

Linear Test Rig

For more information on the linear test rig, refer to GRI Pipeline Simulation Facility Nondestructive Evaluation Laboratory.

Pull Rig Description

The pull rig is a set of four pipe runs through which in-line inspection tools can be pulled. Each pipe run is 300 feet long and contains three 80-foot replaceable defect sections. Mechanical damage and other defect sets are mounted in the replaceable sections and data are taken using the MFL test bed vehicle. Pulls can be made at velocities up to approximately 25 miles per hour.

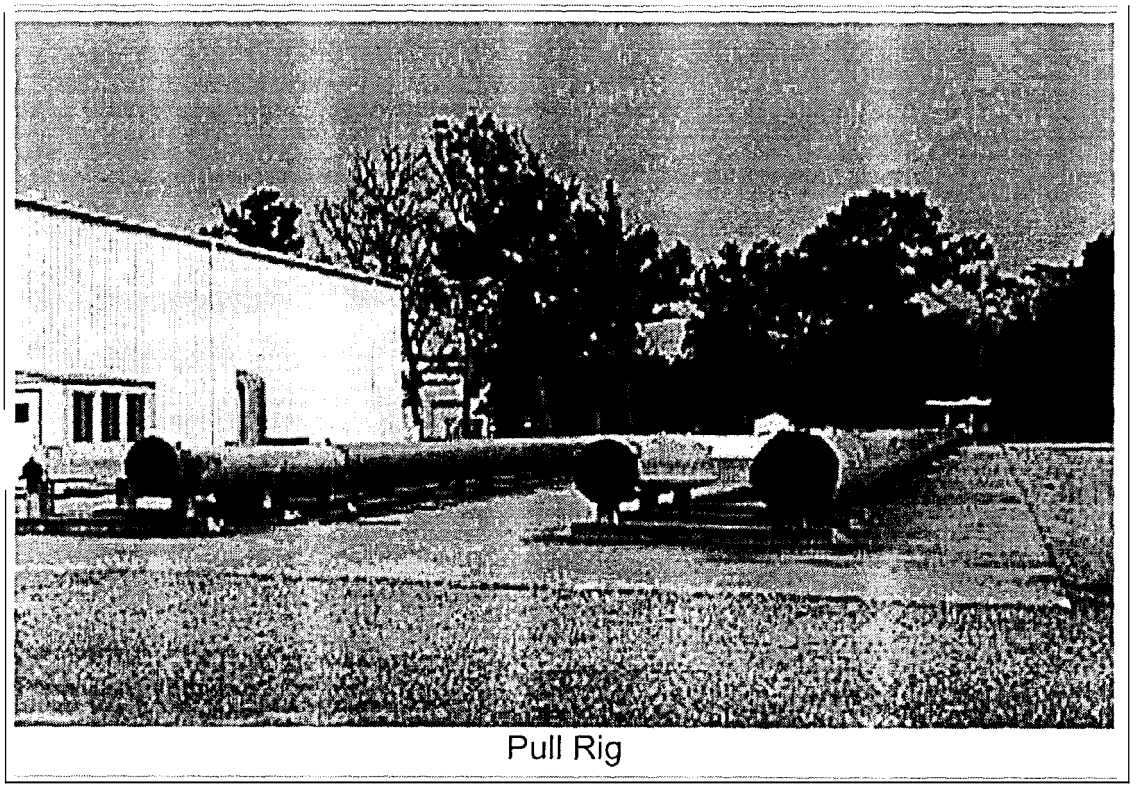

Pull Rig

For more information on the pull rig and its defect sets, refer to GRI Pipeline Simulation Facility Pull Rig, GRI Pipeline Simulation Facility Metal Loss Defect Set, and GRI Pipeline Simulation Facility Stress Corrosion Cracking Defect Set.

Flow loop Description

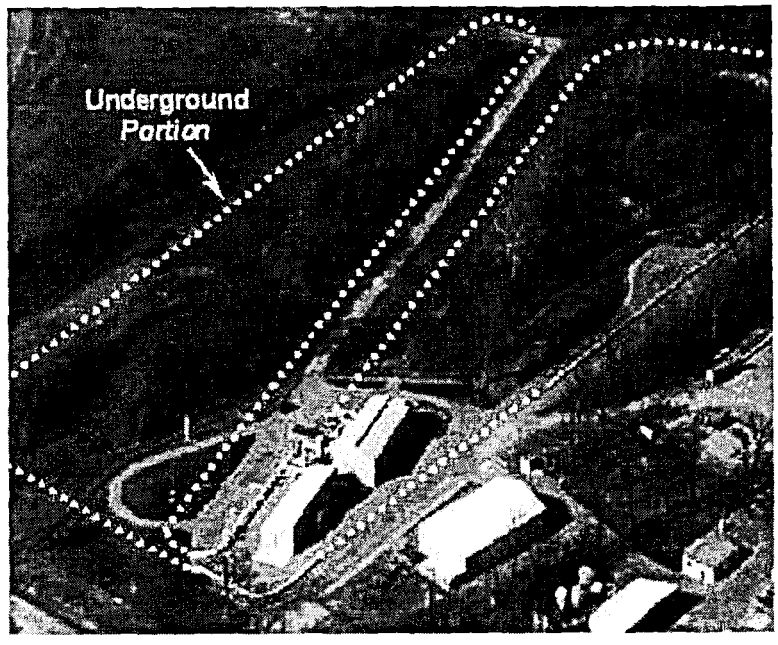

The flow loop is a full-scale pipeline in which testing and development can be conducted on pipeline-related technologies. When used for inspection technologies, it completes the development cycle that starts with small-scale tests and analyses in the linear test rig, and continues through full-scale tests in the unpressurized pull rig. The flow loop fully supports research and development on test bed vehicles or in-line inspection tools under conditions that simulate an operating pipeline without risking the integrity or throughput of an operating line.

The flow loop was designed to meet a number of design requirements that were established by a team of industry advisors and GRI. The resulting layout of the flow loop is shown in the figure. The flow loop is 4,700-foot long and constructed from 24-inch diameter pipe. Both pressure and flow velocity can be controlled to desired set points. Bends, road crossings, an underwater section, and other pipeline features provide a realistic pipeline environment. Known defects have been installed in test sections and other defects, pipe materials, or pipe components can be installed in replaceable sections.

The flow loop provides research and development opportunities in other pipeline areas, such as cathodic protection, pipeline reference temperatures, flow conditions, component performance, and compressor behavior. This section documents some of the general capabilities and major components of the loop to guide the reader in identifying potential development and test opportunities at the flow loop.

General Capabilities

The flow loop provides the following test capabilities:

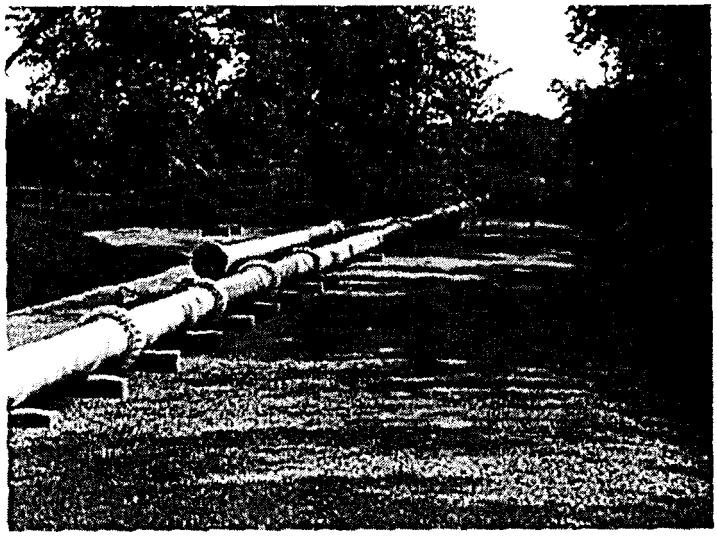

- **Operating pressure** of 200 to 1000 psi.
- **Tool speed** of 2 to over 10 mph (when used for testing inspection equipment, the attainable flow speeds are a function of the pressure differential across the inspection tool).
- **Pressurizing medium of nitrogen** with the possibility of future operation with natural gas.
- **Continuous inspection** tool **movement,** to allow large amounts of data to be generated without retrieving and relaunching the tool, thereby facilitating durability and wear studies.
- **Pressure differential** across **a** tool of at least 10 psi under all operating conditions and up to 80+ psi under some conditions.
- **Removable straight and bend test sections,** which allow different materials and defect sets to be studied.

Description *of* Basic Material Property Testing

An understanding of the effects of stress and strain on magnetic properties for a wide range of materials is needed to determine whether MFL can be used to reliably detect mechanical damage. During the initial planning of the flow loop and as part of Battelle's pipe research program, 40 joints of different pipe materials were removed from service by various pipeline companies and provided to Battelle. These materials had been characterized mechanically for stress-strain and toughness properties and chemically for composition. A total of 36 joints were further characterized magnetically in this project.

The characterization and evaluation had three goals. The first was to determine whether there were clear correlations between magnetic properties and mechanical properties. The second was to determine whether magnetic properties change significantly with the application of tensile or compressive stresses and strains. The final goal was to assemble a database of both magnetic and mechanical properties for future developmental activities. Each of these goals was met.

The 36 samples were magnetically characterized following ASTM Standard A 773-80. This method, illustrated below, uses a ring sample machined to have an outside diameter of 2.0 inches and a square cross section of 0.15 inches. This provides an inside diameter to outside diameter ratio of 85 percent, as required by the ASTM standard. To obtain this sample geometry from the pipe material, a 6-inch by 6-inch coupon was cut from the pipe opposite the seam weld. The 2-inch ring sample was machined from this coupon in a liquid bath to minimize the effect of sample preparation on the magnetic properties.

The ASTM experimental procedure specifies that each ring sample be wound with drive and sense windings. The drive winding, used to generate the magnetic field (H), has a minimum of 140 turns to generate a field strength of 200 Oersted. The sense winding, used to measure the change in flux, has a minimum of 80 turns to attain accurate measurements. The windings were applied by hand, and a few additional turns were added when space was available. Measurements were made using a LDJ model 3500H Hysteresisgraph. Sufficient current was applied to the drive windings to produce 200 Oersted. After demagnetization, the magnetic field and flux density were digitally recorded at increments of nominally 0.2 Oersted for the initial magnetization curve and 0.5 Oersted increments for the hysteresis loop.

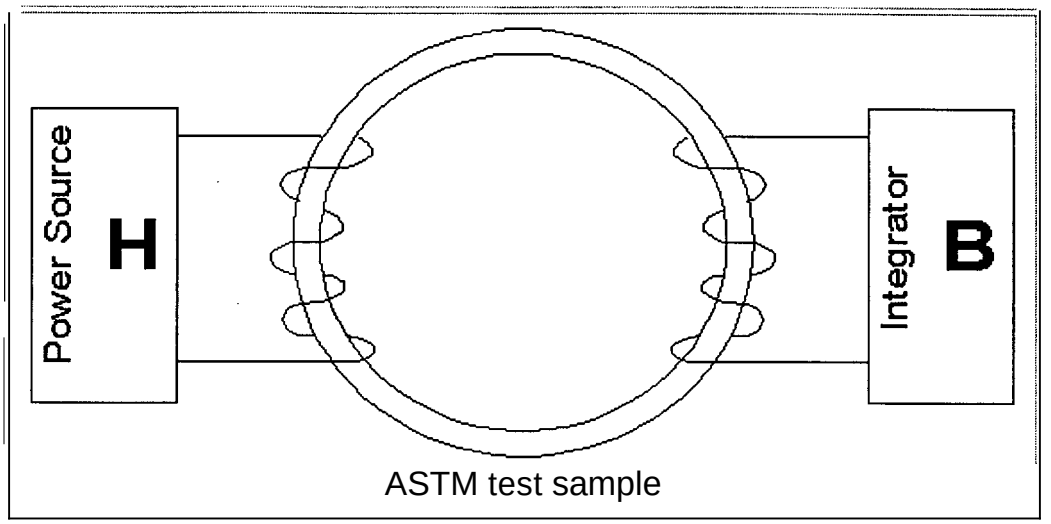
Power Source
H
Integrator
B
ASTM test sample

Description of Material Property Stress Tests

Magnetic properties of 12 of samples were further examined under tensile and compressive loading with up to 8 percent plastic deformation. Two sample configurations were used to measure magnetic properties: a "dogbone" shape for tensile loading and a thin cylinder for compressive loads. The compression sample required special attention to prevent buckling when under load. Two coaxial cylinders were used to support the sample during compression. The central holes in these cylinders were sized so that they could be slipped smoothly over each end of the sample. Very small clearances were used to prevent lateral buckling of the sample. The sensed area, in the center of the sample, was exposed between the larger coaxial cylinders.

Each sample was prepared with strain gages and with an encircling coil to measure magnetic flux. Hall probes in the vicinity of the sensing area were used to measure the magnetizing force. A large magnetizing coil was placed over the whole arrangement, and load cells within the loading linkage were provided as an alternative measure of specimen loading.

Test Procedure

Each sample was mounted in the test fixture, which has a scissors-type loading linkage under manual adjustment. A computer-driven magnetic sensing system automatically cycled the magnetic excitation field and collected the data from all sensors. Strain gages were connected to a bridge circuit and read manually.

B-H curve data were collected for each tensile specimen under a half-dozen different applied loads. Each sample was taken to mechanical yielding, and B-H data were collected again for 1 percent plastic deformation plus a range of applied elastic loads. The sample was then further yielded to 2 percent, and the applied loads were cycled again. The process was repeated to a maximum of 5 to 8 percent plastic deformation. A similar process was carried out with the compressive samples.

Description of Full Pipe Tests

Magnetic properties vary within a pipe. To examine the magnetic properties on a full section of pipe, magnetization curves were measured around the circumference of two pipes under tensile and compressive loading. The following figures shows the arrangement of the test sample.

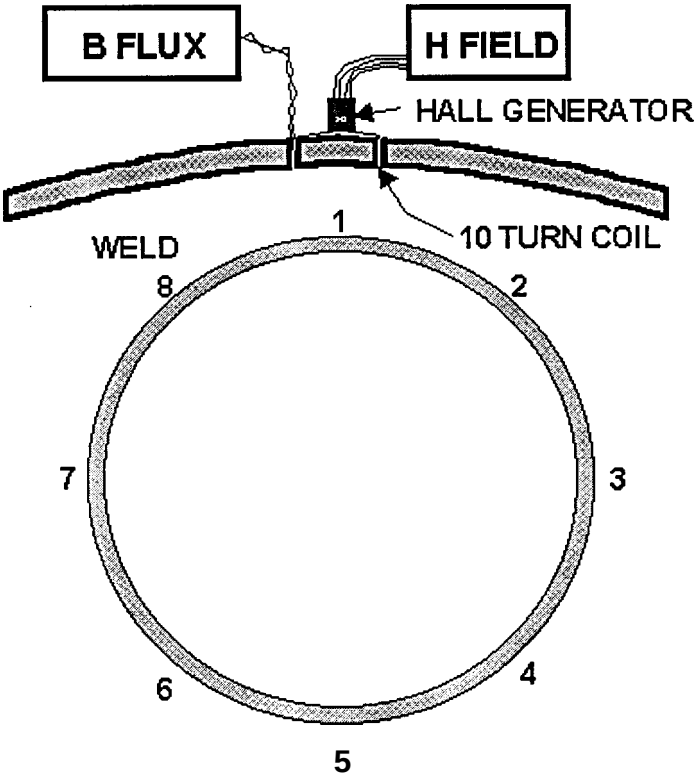

Test Setup for Measuring
Full-Pipe Variations in Stress Effects

Table of Measured Material Property Variations

[COERCIVE FORCE				
	ALL	NO LOAD	TENSION	COMPRESS
MEAN	6.7	7.7	7.4	
Std Dev	1.2	0.55	0.8	
MAX	9	8.6	8.4	10.9
MIN	4.5	7.1	6.3	8.5
MAXIMUM PERMEABILITY				
MEAN	1003	1297	1425	488
Std Dev	331	142	75	28
MAX	2090	1497	1521	549
MIN	580	1101	1325	462

The coercive force is given in Oersteds.
The permeability is given as the maximum relative permeability.

For more detailed information on the magnetic properties of pipeline steels, refer to Variation of Magnetic Properties in Pipeline Steels.

Database of Material Properties

Basic Material and Magnetization Properties

The following table contains data on the magnetization properties for the 36 materials evaluated under this program. Each link provides initial permeability curves, full hysteresis loops, mechanical properties, microstructural information. .

24-06	24-07	24-08	24-09	24-10	24-11	24-13	24-14	24-15	24-17
24-18	24-20	24-21	24-22	24-23	24-27	24-28	24-30	24-31	24-32
24-33	24-34	24-35	24-36	24-37	24-38	24-39	24-40	24-41	24-42
24-43	24-44	24-45	24-46	24-47	24-50				

Magnetization Properties under Tensile and Compressive Loading

The following table contains data on the magnetization properties of twelve of the above materials. These data were taken by Southwest Research Institute. For each material, there are three datasheets. The first shows the magnetization curves for 0%, 1%, and 5% plastic prestrain as a function of stress level. The second shows the permeability curves for 0%, 1%, and 5% plastic prestrain as a function of stress level. The last shows magnetization and permeability curves as a function of plastic strain under conditions of zero loading.

24-06	24-06b	24-06c	24-08	24-08b	24-08c	24-10	24-10b	24-10c	24-11
24-11b	24-11c	24-13	24-13b	24-13c	24-17	24-17b	24-17c	24-18	24-18b
24-18c	24-22	24-22b	24-22c	24-31	24-31b	24-31c	24-35	24-35b	24-35c
24-36	24-36b	24-36c	24-43	24-43b	24-43c				